Journal of Multidisciplinary Healthcare Dovepress

Open Access Full Text Article ORIGINAL RESEARCH

# Clinical-Radiomics Nomogram Model Based on CT Angiography for Prediction of Intracranial Aneurysm Rupture: A Multicenter Study

Xiu-Fen Jia[1,2], Yong-Chun Chen[2], Kui-Kui Zheng[2], Dong-Qin Zhu[2], Chao Chen[2], Jinjin Liu[2], Yun-Jun Yang[2], Chuan-Ting Li[1]

[1]Department of Radiology, Shandong Provincial Hospital, Shandong University, Jinan, 250021, People's Republic of China; [2]Department of Radiology, First Affiliated Hospital of Wenzhou Medical University, Wenzhou, 325000, People's Republic of China

Correspondence: Chuan-Ting Li, Department of Radiology, Shandong Provincial Hospital, Shandong University, 324 Jing Wu Wei-qi Road, Jinan, People's Republic of China, Tel +86 13905319867, Email lichuanting1@126.com



**Objective:** Risk estimation of intracranial aneurysm rupture is critical in determining treatment strategy. There is a scarcity of multicenter studies on the predictive power of clinical-radiomics models for aneurysm rupture. This study aims to develop a clinical-radiomics model and explore its additional value in the discrimination of aneurysm rupture.

**Methods:** A total of 516 aneurysms, including 273 (52.9%) with ruptured aneurysms, were retrospectively enrolled from four hospitals between January 2019 and August 2020. Relevant clinical features were collected, and radiomic characteristics associated with aneurysm were extracted. Subsequently, three models, including a clinical model, a radiomics model, and a clinical-radiomics model were constructed using multivariate logistic regression analysis to effectively classify aneurysm rupture. The performance of models was analyzed through operating characteristic curves, decision curve, and calibration curves analysis. Different models' comparison used DeLong tests. To offer an understandable and intuitive scoring system for assessing rupture risk, we developed a comprehensive nomogram based on the developed model.

**Results:** Three clinical risk factors and fourteen radiomics features were explored to establish three models. The area under the receiver operating curve (AUC) for the radiomics model was 0.775 (95% CI,0.719–0.830), 0.752 (95% CI,0.663–0.841), 0.747 (95% CI,0.658–0.835) in the training, internal and external test datasets, respectively. The AUC for clinical model was 0.802 (95% CI, 0.749–0.854), 0.736 (95% CI, 0.644–0.828), 0.789 (95% CI, 0.709–0.870) in these three sets, respectively. The clinical-radiomics model showed an AUC of 0.880 (95% CI,0.840–0.920), 0.807 (95% CI,0.728–0.887), 0.815 (95% CI,0.740–0.891) in three datasets respectively. Compared with the radiomics and clinical models, the clinical-radiomics model demonstrated better diagnostic performance (DeLong' test $P < 0.05$).

**Conclusion:** The clinical-radiomics model represents a promising approach for predicting rupture of intracranial aneurysms.

**Keywords:** intracranial aneurysm, rupture, computed tomography angiography, radiomics, nomograms

## Introduction

Non-traumatic subarachnoid hemorrhage (SAH) caused by a ruptured aneurysm is a serious neurological disease with high mortality and morbidity.[1] The mortality rate of SAH is approximately 40–50%, and around half of the survivors experience permanent neurological deficits.[2] With advancements in imaging techniques and therapeutic progress, the detection of unruptured aneurysms is becoming more frequent. How to handle these unruptured aneurysms is a dilemma because of the rupture risk and corresponding surgical risk. It is crucial to accurately and promptly screen out patients at high risk of rupture in order to formulate treatment plans.

Therefore, assessing the rupture risk of aneurysms holds significant clinical value for patient treatment and prognosis. The morphology of aneurysms, including the location of aneurysm, shape, as well as size, clinical factors, such as SAH history, smoking, hypertension, gender, population demographics, and hemodynamics, are all risk factors related to the

Received: 15 August 2024
Accepted: 5 December 2024
Published: 10 December 2024

rupture of aneurysms.[3] Currently, computed tomography angiography (CTA) and digital subtraction angiography (DSA) are the main techniques for assessing the risk of aneurysm rupture in clinical settings. CTA is a highly effective diagnostic technique that is not only rapid and cost-efficient, but also boasts widespread accessibility and superior spatial resolution. Compared to DSA (the gold standard for diagnosing intracranial aneurysms), CTA is a non-invasive alternative with broader application.[4] Doctors primarily evaluate the potential for rupture by considering clinical factors of individual patients, along with high-resolution angiographic images. Nevertheless, due to variations in physician experience levels and proficiency, the assessment is highly subjective, leading to inconsistency among experts. Consequently, it is imperative to devise a model for assessing aneurysm rupture risk that can assist doctors in diagnosis and decision-making while avoiding overtreatment or surgical-related risks. Radiomics has been comprehensively applied for the decision making in the medical field, which is defined as converting images into higher-dimensional data, and then mining information from these data to provide better decision support.[5] It involves analyzing and mining numerous quantitative high-dimensional features extracted from medical imaging to objectively and non-invasively assess the lesion and then make the final clinical decision based on key information.[6,7] Radiomics can significantly enhance our comprehension of the significance and clinical relevance of voxel-level imaging phenotypic characteristics in intracranial aneurysms.[8] Previous studies have confirmed that radiomics hybrid models have strong predictive ability for diseases.[9] However, it remains unclear whether radiomics features are superior to clinical risk factors in predicting aneurysm rupture and whether combining them offers additional benefits. Therefore, our aim was to evaluate and compare the predictive capabilities of clinical models, radiomics models and combined clinical-radiomics models in accurately predicting aneurysm rupture. This study established and validated the model based on clinical and radiomics variables collected from the internal cohort. Additionally, the model's accuracy was verified using an entirely independent multicenter validation set, with the objective of characterizing patients who are at a heightened risk of aneurysm rupture.

# Materials and Methods

## Study Population

We conducted a retrospective multicenter investigation, analyzing data from four medical centers, with a specific focused on intracranial aneurysms for which accessible CTA data was available (from January 2019 to August 2020). The study complied to the Declaration of Helsinki and was approved by the ethics committee of First Affiliated hospital of Wenzhou Medical University (YJ2019-027-02). Patient informed consent was waived due to the retrospective design of this study, and patient data confidentiality was protected.

Exclusion criteria were as follows: non-saccular aneurysms (dissecting aneurysms, fusiform aneurysms); Saccular aneurysms accompanied by other vascular diseases, such as arteriovenous malformations, arteriovenous fistulas, Moyamoya disease; Aneurysms that received surgical or interventional treatment before CTA examination.

Eligible patients in our medical center were randomly allocated by a computer-aided algorithms to a training cohort (n = 275, 70%) and an internal validation cohort (n = 119, 30%). These datasets were then binary classified based on whether aneurysm rupture occurred. The external validation datasets (n = 122) encompassed patients from three additional medical centers (Wenzhou Central Hospital, Zhejiang Hospital, and the Second Affiliated Hospital of Wenzhou Medical University).

Clinical data of patients, including sex, age, smoking status (former or current smokers), history of hypertension, history of coronary heart disease, and stroke history were collected. Imaging characteristics of patients were also collected, including the number and location of aneurysms (internal carotid artery; anterior communicating artery; posterior communicating artery; middle cerebral artery; vertebral artery, basilar artery, anterior cerebral artery), as well as whether they had rupture or not. The evaluation criteria for aneurysm rupture are as follows: patients with SAH, aneurysms located near the cerebral pool clot are assessed as ruptured, while aneurysms not located near the cerebral pool clot are judged by DSA; asymptomatic patients without SAH are classified as not ruptured.[10]

## Radiomics Feature Detection

The workflow is illustrated in Figure 1. A neuroradiologist manually performed the segmentation of aneurysm regions of interest (ROIs) on each slice of CTA images through 3D slicer 4.10.1. Subsequently, another neuroradiologist randomly re-segmented 50 of the aneurysms. To assess the inter-observer reproducibility, we computed the inter-class correlation coefficient (ICC). The acquired images were subjected to data preprocessing before extracting radiomics features, considering the variations in CT scanners and their parameters.[11,12] To reduce the variability of radiomics features, we employed image resampling and gray-scale discretization techniques.[13] From each ROI, we extracted 1012 radiomics features. To screen out the most predictive features, we employed the least absolute shrinkage and selection operator

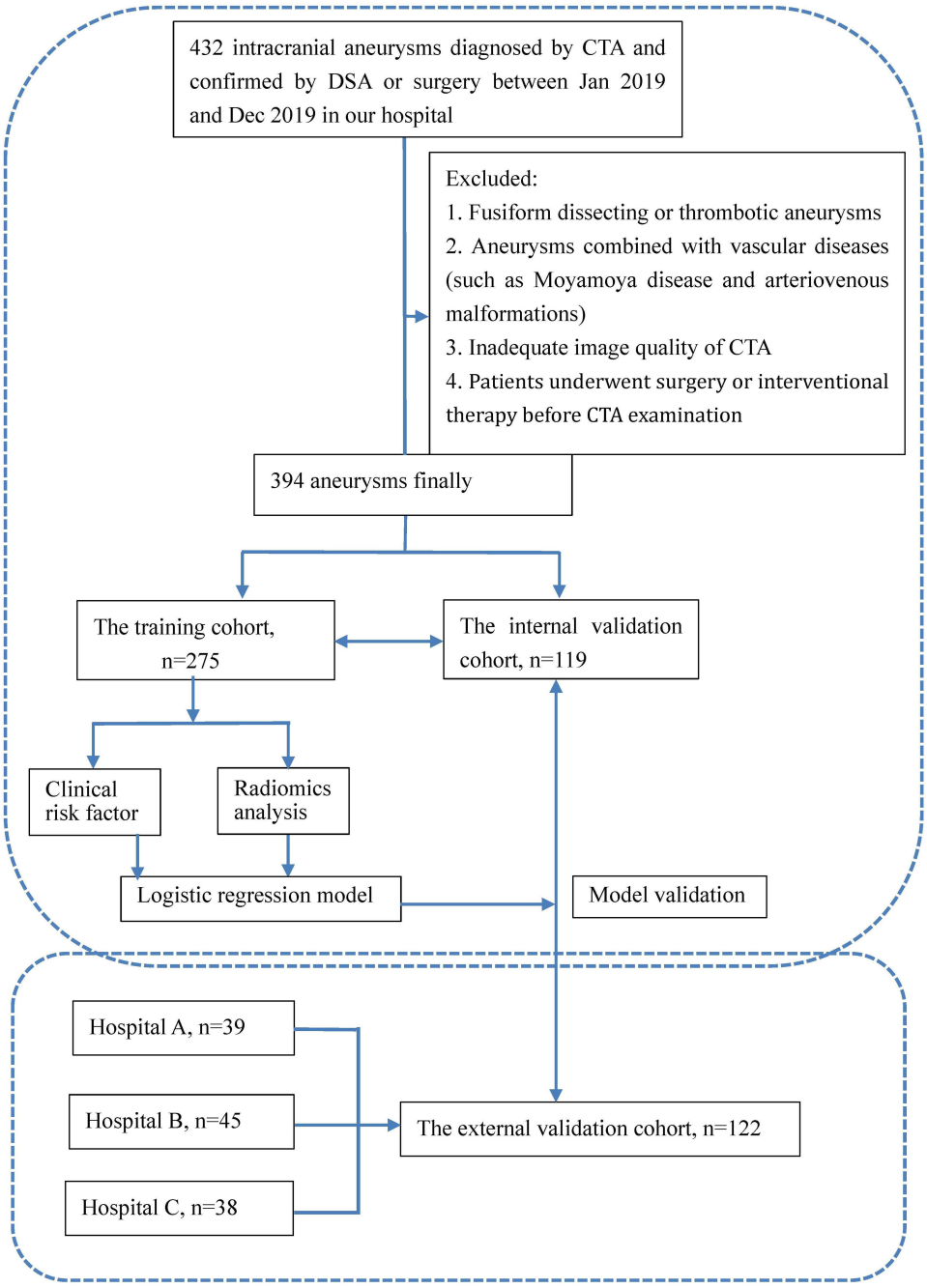


**Figure 1** The flowchart of this study.
**Note**: Hospital (**A**) Zhejiang Hospital. Hospital (**B**) Wenzhou Central Hospital. Hospital (**C**) The second affiliated Hospital of Wenzhou Medical University.

(LASSO) algorithm for dimensionality reduction. We utilized 10-fold cross-validation to develop radiomics model. The radiomics score (Rad-score) for each aneurysm was derived from a linear combination of selected features, with weights assign based on their respective logistic regression coefficient.

## Machine Learning Model Construction

Logistic regression-based machine learning techniques was employed to found a radiomics model using the chosen radiomic features. The predictive accuracy of the radiomics model for aneurysm rupture was evaluated by assessing the Area under the Receiver Operating Characteristic Curve (AUC). The optimal cutoff value was determined based on the maximum Jordan index, and the confusion matrix metrics related to prediction accuracy were calculated, including positive predictive value (PPV), negative predictive value (NPV), specificity and sensitivity. The inter-observer consistency of radiomics features was evaluated using intraclass correlation coefficient (ICC).

## Establishment of Clinical Model and Clinical-Radiomics Model

Clinical data of the ruptured and non-ruptured group were compared in the training cohort. Subsequently, statistically significant factors in univariate analysis were incorporated into a stepwise multiple logistic regression analysis to develop a clinical model that estimate the predicted probability of aneurysm rupture for each patient. The developed clinical model and radiomics scores were utilized as predictive factors in a multiple logistic regression analysis within the training cohort, resulting in the development of a combined model. Finally, the performance of this integrated model was assessed through validation cohorts both internally and externally.

## Construction and Evaluation of Nomograms

To offer an understandable and intuitive scoring system for assessing rupture risk, we created a comprehensive nomogram.[14,15] The discriminative power of the nomogram was assessed by means of ROC curves. Both calibration curves and Hosmer–Lemeshow tests were utilized to assess the concordance between predicted and observed ruptures. The calibration and discrimination of the nomogram were evaluated in both training and validation cohorts.

## Statistical Analysis

The measurement data is represented by ± s and subjected to a single sample Kolmogorov–Smirnov test. If the data conform to a normal distribution, a paired *t*-test is employed for statistical analysis; otherwise, a paired Wilcoxon signed-rank test is used. Count data were statistically analyzed using either the $\chi 2$ test or Fisher's exact probability method. Clinical and radiomics parameters were used to develop clinical model, radiomics model, and clinical-radiomics model. The predictive efficacy of the models was conducted using receiver operating characteristic curve (ROC curve) and calculation of the area under the curve (AUC). The AUCs of different models' ROC curves were compared using the DeLong test. A statistically significant difference was considered when $P < 0.05$. SPSS (version 25) and R (version 3.6.1) were utilized for statistical analysis and model construction.

# Results

## Basic Characteristics

Our study included a total of 516 aneurysm cases, with 275 cases in the training cohort, 119 cases in the internal validation cohort, and 122 cases in the external validation cohort. The mean age of patients experiencing aneurysm rupture was 57.69 ± 11.28 years in the training cohort, 56.14 ± 11.48 years in the internal validation cohort, and 58.61 ± 15.29 years in the external validation cohort.

The incidence of aneurysm rupture was found to be lower among older patients ($P < 0.05$), with rupture rates ranging from 53.5% to 59%. Multiple aneurysms were observed in varying numbers across the three sets, with corresponding rupture rates ranging from approximately 29% to over 65%. Detailed baseline characteristics for each set are provided in Table 1.

**Table 1** Baseline Characteristics of Patients in the Training, Internal Validation and External Validation Dataset

| | Training Cohort (n=275) | | P | Internal Validation Cohort (n=119) | | External Validation Cohort (n=122) | |
|---|---|---|---|---|---|---|---|
| | Unruptured (n=128) | Raptured (n=147) | | Unruptured (n=55) | Raptured (n=64) | Unruptured (n=50) | Raptured (n=72) |
| Age | 64.37±12.51 | 57.69±11.28 | <0.001 | 62.67±12.05 | 56.14±11.48 | 69.08±10.06 | 58.61±15.29 |
| Sex | | | 0.731 | | | | |
| Male | 54(42.2%) | 59(40.1%) | | 24(43.6%) | 29(45.3%) | 23(46.0%) | 22(30.6%) |
| Female | 74(57.8%) | 88(59.9%) | | 31(56.4%) | 35(54.7%) | 27(54.0%) | 50(69.4%) |
| Hypertension | | | 0.018 | | | | |
| Presence | 80(62.5%) | 71(48.3%) | | 31(56.4%) | 22(34.4%) | 35(70.0%) | 33(45.8%) |
| Absence | 48(37.5%) | 76(51.7%) | | 24(43.6%) | 42(65.6%) | 15(30.0%) | 39(54.2%) |
| Smoking | | | 0.287 | | | | |
| Presence | 35(27.3%) | 32(21.8%) | | 10(18.2%) | 12(18.8%) | 16(32.0%) | 13(18.1%) |
| Absence | 93(72.7%) | 115(78.2%) | | 45(81.8%) | 52(81.2%) | 34(68.0%) | 59(81.9%) |
| Coronary artery disease | | | 0.001 | | | | |
| Presence | 1(0.8%) | 1(0.7%) | | 0 | 0 | 13(26.0%) | 18(25.0%) |
| Absence | 127(99.2%) | 146(99.3%) | | 55(100%) | 55(100%) | 37(74.0%) | 54(75.0%) |
| Ischemic stroke | | | 0.158 | | | | |
| Presence | 2(1.6%) | 0(0.0%) | | 2(3.6%) | 2(3.1%) | 7(14.0%) | 3(4.2%) |
| Absence | 126(98.4%) | 147(100.0%) | | 53(96.4%) | 62(96.9%) | 43(86.0%) | 69(95.8%) |
| Multiplicity | | | <0.001 | | | | |
| Presence | 48(37.5%) | 20(13.6%) | | 22(40.0%) | 11(17.2%) | 8(16.0%) | 15(20.8%) |
| Absence | 80(62.5%) | 127(86.4%) | | 33(60.0%) | 53(82.8%) | 42(84.0%) | 57(79.2%) |
| Location | | | <0.001 | | | | |
| ICA | 37(28.9%) | 14(9.5%) | | 8(14.5%) | 39(4.7%) | 18(36%) | 5(6.9%) |
| AcoA | 27(21.1%) | 60(40.8%) | | 16(29.1%) | 27(42.2%) | 8(16%) | 27(37.5%) |
| PcoA | 28(21.9%) | 54(36.7%) | | 17(30.9%) | 17(26.5%) | 15(30%) | 31(43.1%) |
| MCA | 28(21.9%) | 14(9.5%) | | 10(18.2%) | 14(21.9%) | 7(14%) | 6(8.3%) |
| Others | 8(6.2%) | 5(3.5%) | | 4(7.3%) | 3(4.7%) | 2(4%) | 3(4.2%) |

## Construction of Radiomics Scores

The mean ICC value for all radiomics features was calculated as being at a level of significance ($p < 0.05$). Following dimensionality reduction through LASSO regression modeling, we identified and selected a set of fourteen parameters that exhibited high predictive value based on their imaging radiomics scores. In both our internal training and validation groups, it was observed that R-scores were significantly higher among those who experienced ruptures compared to those who did not experience ruptures; thus, indicating R-score's potential as an independent predictor for identifying aneurysms.

## Construction of Clinical Models and Combined Models

After incorporating statistically significant clinical indicators from univariate analysis into multivariate logistic regression analysis, three independent predictive factors for predicting aneurysm rupture were identified: age (OR, 0.934; 95% CI, 0.907–0.961; $p < 0.001$), presence of multiple aneurysms (OR, 0.272; 95% CI, 0.129–0.574; $p = 0.001$), and aneurysm location ($p < 0.001$). A clinical model known as the C-model was developed by incorporating these factors. A combined model called CR-model was subsequently developed by integrating C-model with R-score data, which resulted in improved AUC values when compared against individual models alone within both our training cohort and internal validation cohort. Additionally, we conducted multicenter external cohort validations, which further confirmed CR-

model's superior diagnostic capability over other models such as R-model or C-model alone. The CR-model demonstrated a significantly higher AUC value of 0.880 (95% CI, 0.840–0.920) compared to both the C-model with an AUC of 0.802 (95% CI, 0.749–0.854) and the R-model with an AUC of 0.775 (95% CI, 0.719–0.830) (Figure 2A–C). Similarly, in the internal validation cohort, the AUC value of the CR-model was 0.800 (95% CI, 0.720–0.881), exhibiting a superior performance, while the AUC values of the R-model and C-model were 0.752 (95% CI, 0.663–0.841) and 0.736 (95% CI, 0.644–0.827), respectively. In addition, we conducted independent multicenter external cohort validation, and the AUC value of CR-model was 0.815 (95% CI, 0.740–0.891), surpassing the imaging R-model's AUC values of 0.747 (95% CI, 0.658–0.835). Moreover, the sensitivity, specificity, PPV and NPV associated with the CR-model for predicting aneurysm rupture were 0.776, 0.852, 0.857, and 0.768, respectively. In the internal and external validation cohorts, they were 0.766 and 0.931, 0.764 and 0.560, 0.790 and 0.753, 0.737 and 0.848, respectively. The predictive performance of the three models is detailed in Table 2. After DeLong analysis, it became evident that statistically significant differences existed between CR-Model, R-Model, and C-Model within various cohorts; thus, highlighting superiority possessed by CR-Model especially during external validations.

## Nomogram Construction and Evaluation

Based on this newly established CR-model, a visually represented clinical radiomics nomogram was created with the objective of assessing the risk of aneurysm rupture; Age, presence of multiple aneurysms, location of aneurysms, and R-score were included in the comprehensive nomogram (Figure 3A). Compared with clinical risk factors, R-score accounts for the majority of the scoring system, indicating that quantitative texture parameters play a dominant role in predicting aneurysm rupture. The calibration curve graph drawn exhibits good consistency between nomogram estimation and actual observations. Finally, a decision curve analysis (DCA) was employed to assess the clinical utility of the constructed models at various threshold probabilities in three cohorts (Figure 3B–D). The calibration curves (Figure 2D–F) and Hosmer–Lemeshow test ($p = 0.254$, 0.992, 0.389 in the three cohorts) demonstrate excellent calibration performance.

# Discussion

The rupture of intracranial aneurysms poses a significant risk of mortality and disability. With the popularization of imaging examinations, an increasing number of unruptured aneurysms are being identified. However, controversy remains regarding the necessity for treatment of these unruptured aneurysms due to associated surgical risks. Therefore, the assessment of the risk of rupture in unruptured aneurysms holds significant clinical value. This study retrospectively identified the feasibility of radiomics in predicting intracranial aneurysm rupture. Our research results indicate a close correlation between CTA-based radiomics scores and the rupture of aneurysms. The combined model of R-model and C-models has significantly better predictive performance for aneurysm rupture than simple C-model and R-models, and has greater advantages in evaluating the risk of aneurysm rupture.

Radiomics initially played a significant clinical role in tumor assessment,[16–18] and due to its ability to quantify lesion heterogeneity, it has gradually been applied in the evaluation of cerebrovascular diseases in recent years. Ruptured aneurysms exhibit distinct radiological characteristics compared to unruptured aneurysms. Leveraging radiomic features, particularly structural ones, can significantly enhance the predictive performance of aneurysm rupture.[19] Consistent with previous research, the R-score established in this study's training set, internal and external validation set reliably assesses the risk of aneurysm rupture (with AUC values of 0.775, 0.752, and 0.747, respectively). The present study rigorously selected 14 out of 1012 radiomics features, which were found to be highly predictive, in order to construct a robust radiomics model, thereby further demonstrating the potential of radiomics features in aneurysm rupture prediction, aligning with previous studies.[8] Among numerous radiomics features, features that display image heterogeneity (such as ShortRunHighGreyLevelEmphasis, SmallDependenceHighGreyLevelEmphasis, etc) are selected. Radiomics describes the morphology and texture features of aneurysms from a microscopic perspective, so texture analysis can indirectly reflect the heterogeneity within aneurysms.[20,21] The texture features inside the aneurysm cavity are likely due to uneven distribution of contrast agents, which is believed to be associated with turbulent blood flow. Turbulence in blood flow may activate inflammatory mechanisms, leading to a high risk of rupture.[1] This suggests that these texture patterns may

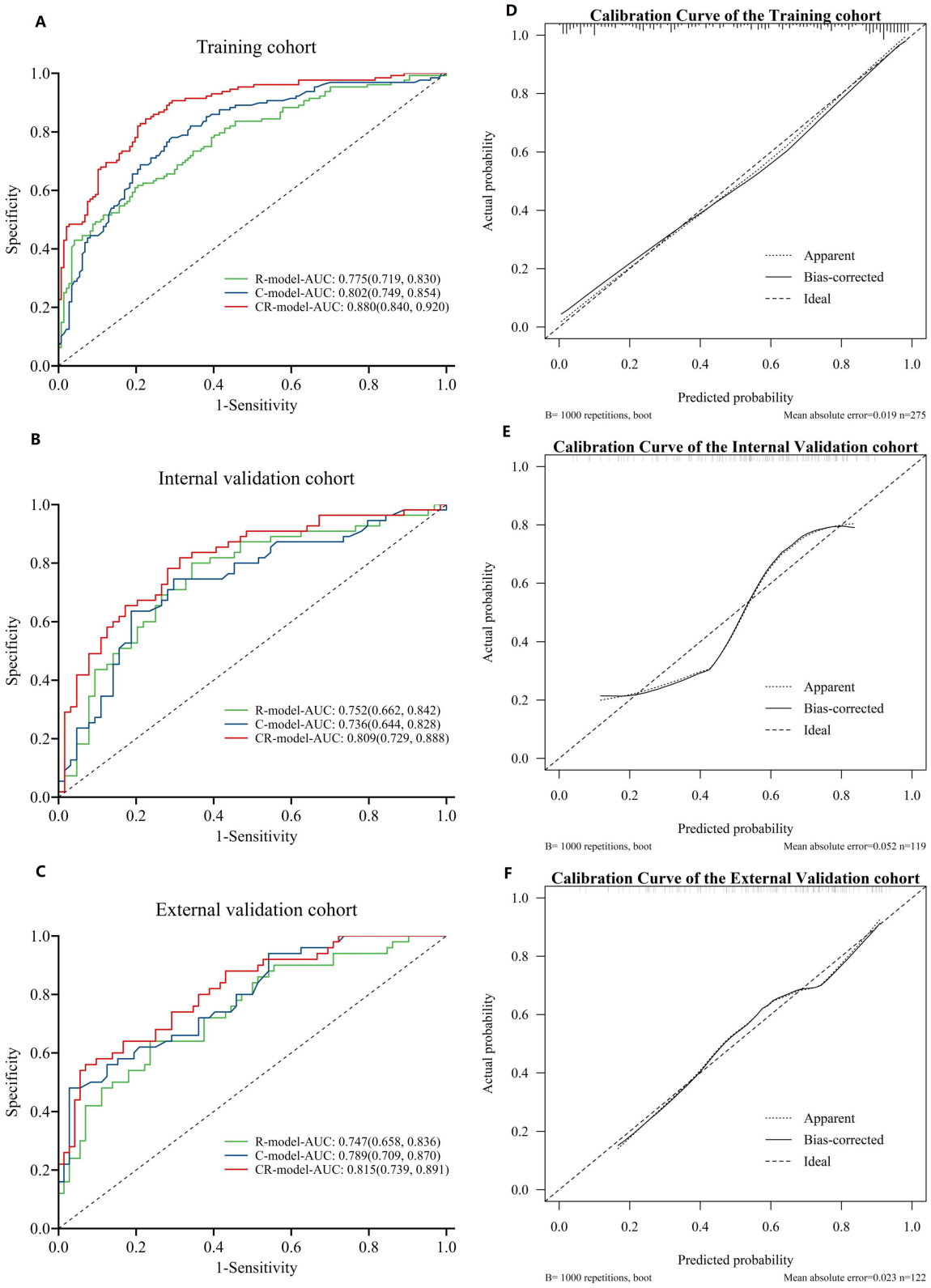


**Figure 2** Receiver operating characteristic (ROC) curves and calibration curve of the radiomics model (R model), clinical model (C model), and clinical radiomics model (CR model). The operating characteristic curves of the three models in the training (**A**) and internal validation cohort (**B**) external validation cohort (**C**). Calibration curve of the three models in the training (**D**), internal validation and external validation cohorts (**E** and **F**).

**Table 2** Performance of the Radiomics, Clinical and Clinical-Radiomics Models

| Datasets | Models | AUC (95% CI) | ACC | SEN | SPE | PPV | NPV |
|---|---|---|---|---|---|---|---|
| Training cohort | R-model | 0.775(0.719, 0.830) | 0.713 | 0.796 | 0.617 | 0.705 | 0.725 |
| | C-model | 0.802(0.749, 0.854) | 0.742 | 0.707 | 0.781 | 0.788 | 0.699 |
| | CR-model | 0.880(0.840, 0.920) | 0.807 | 0.776 | 0.844 | 0.851 | 0.766 |
| Internal validation Cohort | R-model | 0.752(0.662, 0.842) | 0.723 | 0.656 | 0.8 | 0.792 | 0.667 |
| | C-model | 0.736(0.644, 0.828) | 0.731 | 0.812 | 0.636 | 0.722 | 0.745 |
| | CR-model | 0.807(0.728, 0.887) | 0.748 | 0.688 | 0.818 | 0.815 | 0.692 |
| External validation Cohort | R-model | 0.747(0.658, 0.836) | 0.713 | 0.764 | 0.64 | 0.753 | 0.653 |
| | C-model | 0.789(0.709, 0.870) | 0.77 | 0.972 | 0.48 | 0.729 | 0.923 |
| | CR-model | 0.815(0.740, 0.891) | 0.779 | 0.931 | 0.56 | 0.753 | 0.848 |

**Abbreviations**: R-model, radiomics model; C-model, clinical model; CR-model, clinical-radiomics model; AUC, area under the receiver operating curve; ACC, accuracy; CI, confidence interval; PPV, positive predictive value; NPV, negative predictive value; SEN, sensitivity; SPE, specificity.

serve as indicators of the hemodynamics within the aneurysm, which are closely associated with aneurysm rupture. This further underscores the rationale for considering radiomics texture features as potential risk factors in assessing aneurysm rupture.

In practice, some risk factors have been associated with the development and rupture of intracranial aneurysms. These encompass patient demographics such as age and gender, lifestyle choices including smoking and alcohol consumption,

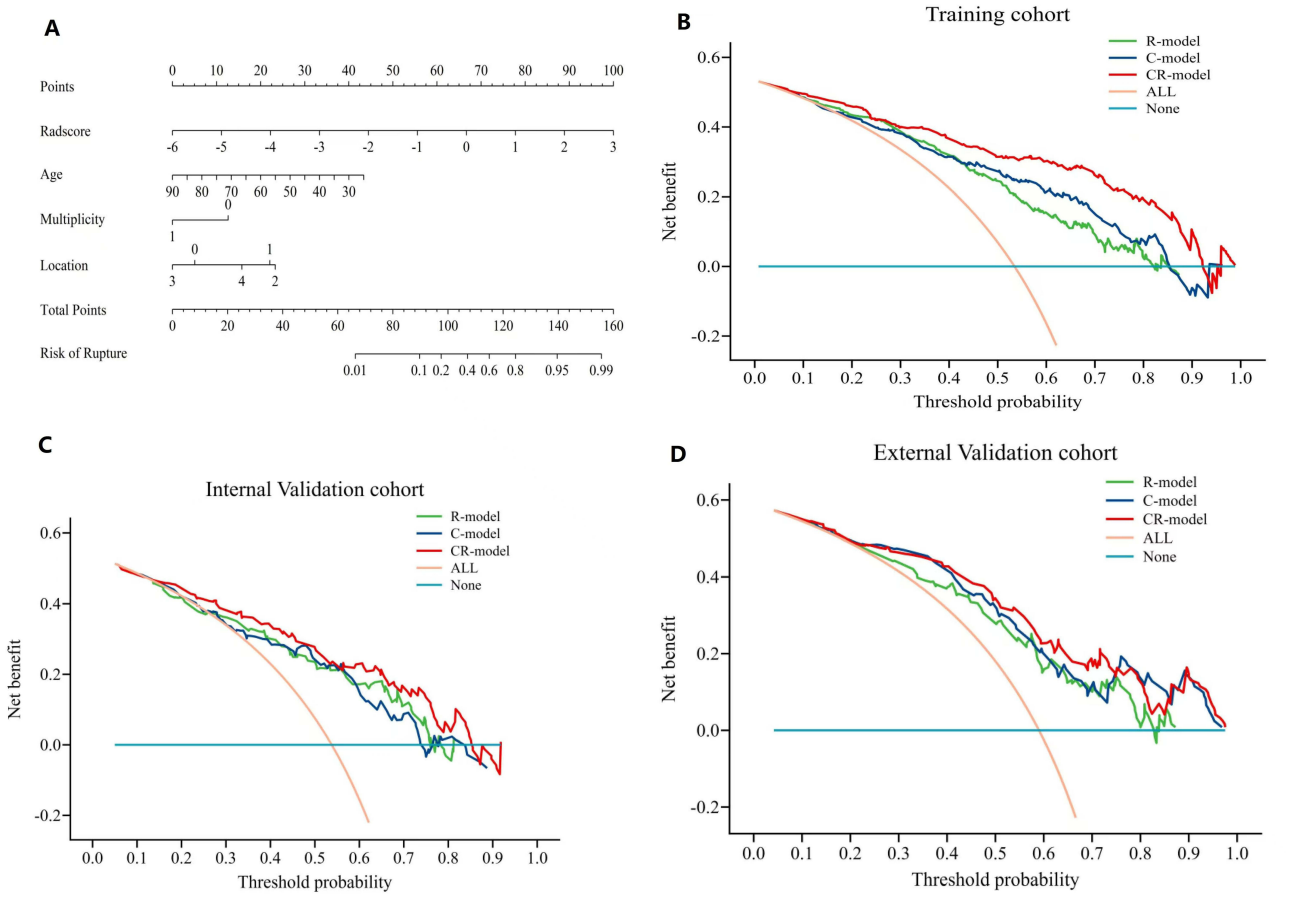


**Figure 3** Decision curve analysis and comprehensive nomogram for intracranial aneurysms in all patients. (**A**) Nomogram for the prediction of small aneurysm ruptures; decision curve analysis of the clinical model, radiomics model, and clinical–radiomics model with the threshold probability on the x-axis and the net benefit on the y-axis in the (**B**) training cohort, (**C**) internal validation cohort, and (**D**) external validation cohort.

family history, previous stroke incidents, hypertension history, as well as characteristics of the aneurysm itself such as size, location, and shape. The variations in research outcomes primarily stem from disparities within the study populations.[22–25] In our study, patient age, the presence of multiple aneurysms, as well as location of aneurysms were statistically significant in predicting lesion rupture. Recently, Alwalid et al[1,8,19] compared the diagnostic performance of CTA-based radiomics models and traditional radio-morphological models for predicting aneurysm rupture. The results confirmed that radiomics models have better diagnostic performance and are a reliable and objective auxiliary diagnostic technique. In this study, the diagnostic efficacy of radiomics model was comparable to the C-model, yet the combined model (AUC: 0.880) significantly surpassed the standalone clinical model (AUC: 0.802), highlighting the substantial contribution of the radiomics model to the combined model's construction. The advantage of our research lies in the addition of multicenter external validation, in addition to internal validation, which confirms the robustness and reproducibility of our CR-model. In addition, we have developed a straightforward and visually intuitive intracranial aneurysm rupture risk scoring system, utilizing a nomogram.

The study is subject to certain limitations. First, it is a retrospective, cross-sectional study, which may pose a risk of selection bias. Second, while radiomics calculations are automated, ROI segmentation is semi-automatic and is susceptible to manual errors, which hinders the clinical application of radiomics. Third, we did not consider the history of recent bleeding because those with recent bleeding are rare. Lastly, the images in the external validation dataset are sourced from various scanning protocols and machines, potentially influencing the validation outcomes.

## Conclusion

In conclusion, we conducted an analysis of intracranial aneurysm rupture using clinical and radiomics data from multiple centers. The discovery of our study suggests that radiomics features derived from CTA can independently predict the risk of arterial aneurysm rupture. Moreover, the inclusion of both radiomics features and clinical risk factors in the CR-model significantly enhances the diagnostic accuracy for predicting aneurysm rupture. Compared to the C-model, CR-model that includes both radiomics features and clinical risk factors significantly improves the diagnostic efficacy for predicting arterial aneurysm rupture. This approach can serve as a complementary tool to standard imaging examinations, enabling accurate and timely identification of high-risk patients and facilitating personalized treatment planning by clinicians.

## Disclosure

The authors report no conflicts of interest in this work.

## References


1. An X, He J, Di Y, et al. Intracranial aneurysm rupture risk estimation with multidimensional feature fusion. *Front Neurosci*. 2022;16:813056. doi:10.3389/fnins.2022.813056
2. Boulouis G, Rodriguez-Régent C, Rasolonjatovo EC, et al. Unruptured intracranial aneurysms: an updated review of current concepts for risk factors, detection and management. *Rev Neurol*. 2017;173(9):542–551. doi:10.1016/j.neurol.2017.05.004
3. Abboud T, Rustom J, Bester M, et al. Morphology of ruptured and unruptured intracranial aneurysms. *World Neurosurg*. 2017;99:610–617. doi:10.1016/j.wneu.2016.12.053
4. Philipp LR, McCracken DJ, McCracken CE, et al. Comparison between CTA and digital subtraction angiography in the diagnosis of ruptured aneurysms. *Neurosurgery*. 2017;80(5):769–777. doi:10.1093/neuros/nyw113
5. Robert JG, Kinahan PE, Hricak H. Radiomics: images are more than pictures, they are data. *Radiology*. 2015;278.
6. Mayerhoefer ME, Materka A, Langs G, et al. Introduction to radiomics. *J Nucl Med*. 2020;61(4):488–495. doi:10.2967/jnumed.118.222893
7. Limkin EJ, Sun R, Dercle L, et al. Promises and challenges for the implementation of computational medical imaging (radiomics) in oncology. *Ann Oncol*. 2017;28(6):1191–1206.
8. Alwalid O, Long X, Xie M, et al. CT angiography-based radiomics for classification of intracranial aneurysm rupture. *Front Neurol*. 2021;12:619864. doi:10.3389/fneur.2021.619864
9. Hu T, Wang S, Huang L, et al. A clinical-radiomics nomogram for the preoperative prediction of lung metastasis in colorectal cancer patients with indeterminate pulmonary nodules. *Eur Radiol*. 2019;29(1):439–449. doi:10.1007/s00330-018-5539-3
10. Shi Z, Chen GZ, Mao L, et al. Machine learning-based prediction of small intracranial aneurysm rupture status using CTA-derived hemodynamics: a multicenter study. *Am J Neuroradiol*. 2021;42(4):648–654. doi:10.3174/ajnr.A7034
11. Morin O, Vallières M, Jochems A, et al. A deep look into the future of quantitative imaging in oncology: a statement of working principles and proposal for change. *Int J Radiat Oncol Biol Phys*. 2018;102(4):1074–1082. doi:10.1016/j.ijrobp.2018.08.032
12. Chen Q, Xia T, Zhang M, et al. Radiomics in stroke neuroimaging: techniques, applications, and challenges. *Aging Dis*. 2021;12(1):143–154. doi:10.14336/AD.2020.0421

13. Shafiq-Ul-Hassan M, Latifi K, Zhang G, et al. Voxel size and gray level normalization of CT radiomic features in lung cancer. *Sci Rep*. 2018;8(1):10545. doi:10.1038/s41598-018-28895-9
14. Balachandran VP, Gonen M, Smith JJ, DeMatteo RP. Nomograms in oncology: more than meets the eye. *Lancet Oncol*. 2015;16(4):e173–e180. doi:10.1016/S1470-2045(14)71116-7
15. Glasser L, Doerfler R. A brief introduction to nomography: graphical representation of mathematical relationships. *Int J Math Educ Sci Technol*. 2018;50(8):1273–1284. doi:10.1080/0020739X.2018.1527406
16. Liu Z, Wang S, Dong D, et al. The applications of radiomics in precision diagnosis and treatment of oncology: opportunities and challenges. *Theranostics*. 2019;9(5):1303–1322. doi:10.7150/thno.30309
17. Lambin P, Leijenaar RT, Deist TM, et al. Radiomics: the bridge between medical imaging and personalized medicine. *Nat Rev Clin Oncol*. 2017;14(12):749–762. doi:10.1038/nrclinonc.2017.141
18. Gillies RJ, Kinahan PE, Hricak H. Radiomics: images are more than pictures, they are data. *Radiology*. 2016;278(2):563–577. doi:10.1148/radiol.2015151169
19. Ou C, Chong W, Duan C-Z, et al. A preliminary investigation of radiomics differences between ruptured and unruptured intracranial aneurysms. *Eur Radiol*. 2021;31(5):2716–2725. doi:10.1007/s00330-020-07325-3
20. Xu X, Zhang H-L, Liu Q-P, et al. Radiomic analysis of contrast-enhanced CT predicts microvascular invasion and outcome in hepatocellular carcinoma. *J Hepatol*. 2019;70(6):1133–1144. doi:10.1016/j.jhep.2019.02.023
21. Zhu D, Chen Y, Zheng K, et al. Classifying ruptured middle cerebral artery aneurysms with a machine learning based, radiomics-morphological model: a multicentral study. *Front Neurosci*. 2021;15:721268. doi:10.3389/fnins.2021.721268
22. Thompson BG, Brown RD, Amin-Hanjani S, et al. Guidelines for the management of patients with unruptured intracranial aneurysms: a guideline for healthcare professionals from the American Heart Association/American Stroke Association. *Stroke*. 2015;46(8):2368–2400. doi:10.1161/STR.0000000000000070
23. Steiner T, Juvela S, Unterberg A, et al. European Stroke Organization guidelines for the management of intracranial aneurysms and subarachnoid haemorrhage. *Cerebrovasc Dis*. 2013;35(2):93–112. doi:10.1159/000346087
24. Ishibashi T, Murayama Y, Urashima M, et al. Unruptured intracranial aneurysms: incidence of rupture and risk factors. *Stroke*. 2009;40(1):313–316. doi:10.1161/STROKEAHA.108.521674
25. Feng J, Zeng R, Geng Y, et al. Automatic differentiation of ruptured and unruptured intracranial aneurysms on computed tomography angiography based on deep learning and radiomics. *Insights Imaging*. 2023;14:76. doi:10.1186/s13244-023-01423-8